Geometry of the Myosin Dimer in High-Salt Media. II. Hydrodynamic Studies on Macromodels of Myosin and Its Rod Segments†

Morris Burke and William F. Harrington*

ABSTRACT: Rotary frictional experiments on macromodels corresponding to monomer and dimer structures of myosin, light meromyosin (LMM), and the entire rod section of myosin (rod) are described. The rotational frictional coefficients for these macromodels have been evaluated and for the single rods show good agreement between experiment and the expected value based on the Broersma equation. The rotational frictional coefficients for the rod dimers have been found to be closely similar to that predicted by the Broersma equation for an equivalent cylinder of length and volume equal to the dimer. This finding enables empirical equations to be developed in which the degree of overlap occurring in the dimer can be related to its intrinsic viscosity. The degree of overlap occurring in the LMM and rod dimers may be calculated from the intrinsic viscosity of the dimer species derived from η_{sp}/c *vs.* c data. This result is consistent with assigning a parallel geometry to the myosin dimer in high-salt media. A hydrodynamic analysis of the rotary friction data obtained from torque measurements on macromodels of myosin in the monomer and dimer states is also described.

In the previous paper (Harrington and Burke, 1972), evidence from high-speed equilibrium sedimentation and from viscosity studies was presented to show that, like myosin, the rod segments light meromyosin (LMM) and "rod," associate reversibly to form dimers. Analysis of the reduced viscosity *vs.* concentration dependence of these three particles indicates that in all cases the dimeric structure is of higher asymmetry than that of the parent monomer. Moreover, from the deduced value of the intrinsic viscosity of the dimer and its molecular weight it was possible to obtain an estimate of the length of the dimer, provided we assume that the hydrodynamic properties of the dimer can be mimicked by an equivalent prolate ellipsoid. This assumption is probably valid in the case of the monomeric particles but its extension to the dimeric case is uncertain and further, its use for monomeric or dimeric myosin is not valid due to the nonuniform mass distribution of these molecules.

In the present study, we describe rotary frictional experiments on macromodels corresponding to monomeric and dimeric LMM, rod, and myosin. We will demonstrate that in the case of the rod-like particles it is possible to derive an empirical relationship between the intrinsic viscosity of the dimer and its geometrical configuration. These findings show that the assumption of hydrodynamic equivalence of the dimer to an equivalent prolate ellipsoid is a very good approximation. Our results are consistent with an arrangement of myosin monomers in the dimer species in parallel-type geometry.

Materials and Methods

Precision ground stainless steel shaft and stainless steel balls were puchased from Small Parts Inc. (Miami, Fla.). Brass rods were purchased from Brass and Copper Supply Co. (Baltimore, Md.). Rotary friction experiments were performed with a device similar to that employed by Kuhn and Kuhn (1952), shown schematically in Figure 1. A cylindrical vat, V, (38.5 cm diameter, 28.0 cm height) was filled with a solution of invert sugar, the viscosity of which (η = 500 poise, 21°) was obtained by measuring the rate of descent of stainless steel balls ($^3/_{32}$ and $^1/_{16}$ in. diameter) through the solution near the center of the vat, thus evaluating the translatory frictional resistance. For this purpose, the rate of descent of the ball was measured by focusing a cathetometer simultaneously on the ball and on a rigidly mounted, precision stainless steel ruler with $^1/_{64}$-in. subdivisions. Stokes' law was found to be accurately obeyed and the viscosity of the bath was calibrated before and after each rotational experiment. The rotational frictional resistance of the vertical spindle, A (diameter 0.3174 cm), was obtained from measurements of the angular velocity at constant torque for two spheres (0.375 and 0.5 in. diameter), assuming the rotational frictional coefficient of the sphere to be $\zeta_0 = 8\pi\eta r^3$; it was found to be less than 0.5% of the measured torques of the molecular models which ranged from 19,600 to 58,800 dyne cm. Rotational frequencies of the order 0.01 rps and lower were employed for the macromodels. Reynolds numbers were below the critical range for turbulent flow and wall effects were found to contribute less than 1% for all but the longest structures which were estimated (see Haltner and Zimm, 1959) to yield an uncertainty of about 2%. This was verified by rotary experiments on single rods (see "Results" section).

For the purposes of this study, it was assumed that LMM and rod are rigid rods with lengths equal to 860 and 1290 Å, respectively, and diameter of 20 Å. Macromodels corresponding to monomeric and dimeric LMM and rod structures were constructed from precision ground stainless steel and brass rods of diameters 0.3174 and 0.236 cm, respectively. The macromodels were drilled and tapped to accept the threaded lower end of the vertical spindle, A, which was used to suspend the macromodels in the viscous liquid. A 2.0-cm radius pulley, B, was attached to the spindle near the upper end

† Contribution No. 674 from the Department of Biology, McCollum-Pratt Institute, The Johns Hopkins University, Baltimore, Maryland. *Received December 13, 1971.* This investigation was supported by U. S. Public Health Service Grant No. AM 04349-12. One of us (M. B.) gratefully acknowledges a Muscular Dystrophy Associations of America postdoctoral fellowship.

and the spindle, A, was mounted on a rigid, moveable platform between two ball bearings, C. The spindle was rotated by means of a thread which passed around the pulley, thence over a larger pulley, D, of 5.0-cm radius with axis normal to the spindle. Balance weights (20–30 g) were attached to the thread to exert the required torque. The dimeric structures, M, were constructed by placing two monomeric rods side by side with the required amount of overlap in a metal jig with a rectangular slot exactly twice the diameter of the single rod and the rod structures were fused together by applying a minimum amount of solder along the line of contact. All rod structures possessed hemispherical (rounded-off) ends. Macromodels representing the monomeric myosin molecule were constructed assuming the particle to be a rigid rod 1290 Å in length and diameter 20 Å attached to a sphere of volume equal to that of the rod. To construct the myosin dimer model without distortion of the rod segment a hole was drilled through the spherical head of one unit allowing the rod section of a second monomer unit to pass through and lie directly alongside the rod segment of the original unit. For each LMM and rod dimer, torque measurements were carried out on two models representing configurations where the large semi-minor axis was in the horizontal and the vertical plane. In all cases, torques for these configurations were found to be identical within 1%. The harmonic mean is tabulated in each case.

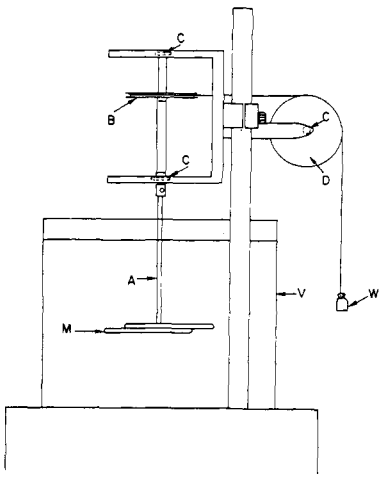

FIGURE 1: Schematic diagram of the hydrodynamic apparatus employed for the rotary frictional measurements. See Materials and Methods for detailed description.

Results

Viscosity Behavior of Rod-Like Solutes Undergoing Reversible Dimerization. Although the intrinsic viscosity of a protein is a sensitive measure of particle asymmetry, the application of viscosity techniques to study associating systems has not received much attention. If a spherical, globular protein is associating to form compact, spherical structures there will be no change in the intrinsic viscosity. If, on the other hand, the association proceeds through the formation of an asymmetric structure, then the intrinsic viscosity of such a system should increase. In this connection, Reisler and Eisenberg (1970), in their elegant study on the association behavior of bovine glutamate dehydrogenase, were able to demonstrate that the concentration-dependent association of this protein to form elongated structures is readily detected by viscometry.

Consider the hydrodynamic behavior of very asymmetric solutes undergoing reversible association of the monomer $\rightleftharpoons$ dimer type. From the development presented in part I (Harrington and Burke, 1972) it is clear that the reduced viscosity of such a system may be defined by the following equation

$$\eta_{sp}/c = ([\eta]_m + k'[\eta]_m^2 c_m)c_m/c + ([\eta]_d + k'[\eta]_d^2 c_d)\, c_d/c \quad (1)$$

where the symbols have the same meaning as described in part I and the relationships between c_m, c_d, and total concentration, c, are given by eq 2a and 2b

$$c_m + c_d = c \quad (2a)$$

$$K_2 = c_d/c_m^2 \quad (2b)$$

Provided the dimer species is significantly more asymmetric than the monomer, the general form of the reduced viscosity, η_{sp}/c *vs.* concentration dependence will be of the type shown in Figure 2a, which shows a family of curves obtained by assigning invariant values of 1.0 and 2.0 dl per g for $[\eta]_m$ and $[\eta]_d$ in eq 1, respectively, and varying the equilibrium constant for dimerization. A value of 0.45 was assigned to the dimensionless Huggins' constant, k', assumed the same for monomer and dimer, since this is a value common to many nonassociating systems. Under these conditions the reduced viscosity will increase monotonically with increasing concentration and approach a slope of $k'[\eta]_d^2$ at high concentration. When the intrinsic viscosity of dimer is appreciably lower than monomer, the reduced viscosity will decrease with increasing concentration in the low concentration range, pass through a minimum and again approach a slope of $k'[\eta]_d^2$ at high concentration. This situation is depicted in Figure 2b for various values of the equilibrium constant, K_2, and assigned values of $[\eta]_m$ and $[\eta]_d$ of 1.0 and 0.65 dl per g, respectively.

The distinguishing feature of the plots shown in Figure 2 is the marked sensitivity of the reduced viscosity profile to the asymmetry of the dimer species, thus providing a powerful analytic technique for establishing the geometry of the dimer.

Figure 3 demonstrates the effect of varying the dimer asymmetry $[\eta]_d$ on the reduced viscosity *vs.* concentration plots for fixed $[\eta]_m$ equal to 1.0 dl/g and an association constant, K_2 of 10 dl/g. In the situation where the dimer has the same asymmetry as the monomer ($[\eta]_d = [\eta]_m$) eq 1 simplifies to give

$$\eta_{sp}/c = [\eta]_m + k'[\eta]_m^2 \left(\frac{2c_m^2 - 2c_m c + c^2}{c}\right) \quad (3)$$

The η_{sp}/c *vs.* c profile for this special case where $K_2 = 10$ dl/g is also shown in Figure 3.

Although the plots shown in Figures 2 and 3 may be employed to demonstrate the relationship between the asymmetries of monomer and dimer, they are clearly of limited use unless the intrinsic viscosity of the dimer can be related to a particular dimer geometry. In the following section this relationship will be established.

Rotary Frictional Experiments. We have utilized the experimental approach of Kuhn and Kuhn (1952), Haltner and Zimm (1959), Broersma (1960), and Reisler and Eisenberg (1970) to determine the torques required to rotate macroscopic models corresponding to monomeric and dimeric rod structures of various geometries. The torque required to rotate such a model with unit angular velocity in a viscous fluid

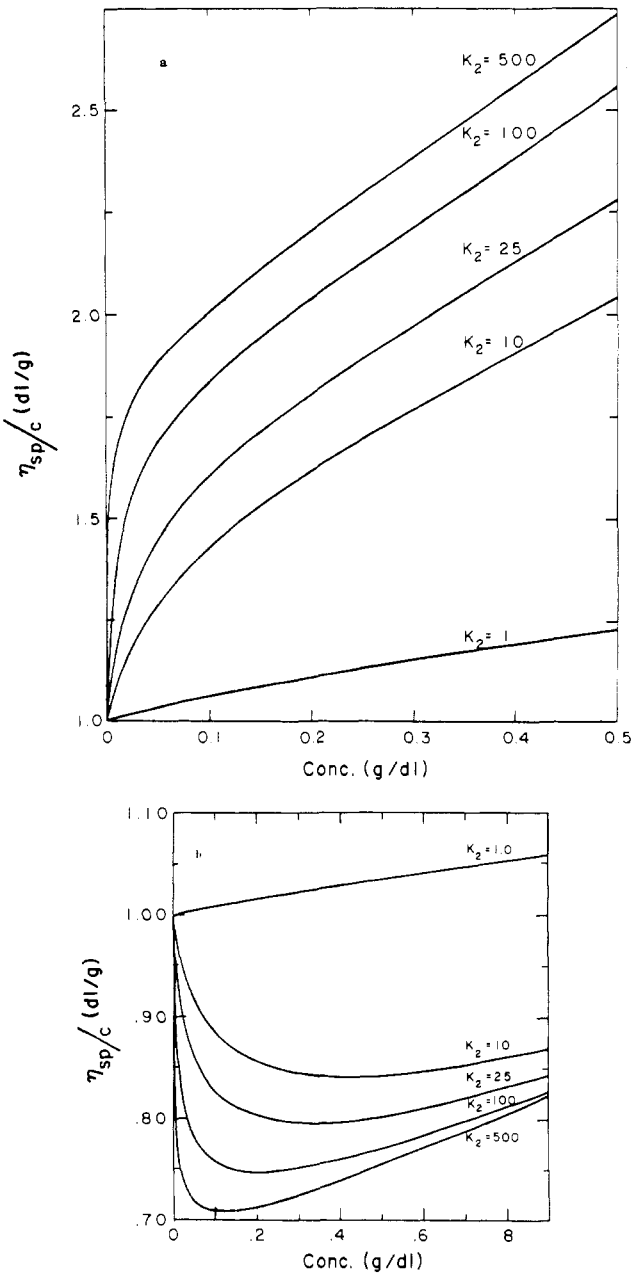

FIGURE 2: Simulated reduced viscosity *vs.* concentration profiles for a rod-like solute undergoing a monomer $\rightleftharpoons$ dimer association. (a) The intrinsic viscosities of monomer and dimer are held constant at 1.0 and 2.0 dl/g, respectively, and the equilibrium constant K_2 is assigned the values shown. The Huggins constant (k') is assumed to be 0.45 for both monomer and dimer. (b) The intrinsic viscosities of monomer and dimer are held constant at 1.0 and 0.65 dl/g, respectively, and the equilibrium constant assigned the values shown. The Huggins constant (k') is assumed to be 0.45 for both monomer and dimer.

about an axis through the center of gravity and perpendicular to the long axis of the rod, is by definition, the rotational frictional coefficient, ζ, of the structure about this axis of rotation. Exact solutions relating the rotational frictional coefficient to the geometry of solute particles are known only for the sphere and ellipsoids of revolution. The approximate treatment of Burgers (1938) to estimate the rotational frictional coefficient of cylinders has been shown to be inadequite by Broersma (1960) and by Haltner and Zimm (1959). Broersma has derived an alternate theoretical expression for

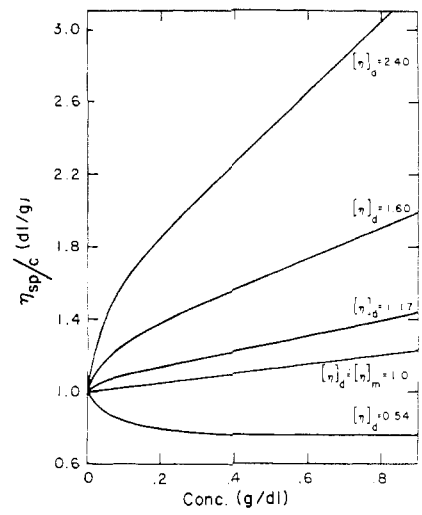

FIGURE 3: The effect of the dimer asymmetry $[\eta]_d$ on the reduced viscosity *vs.* concentration profile for a rod-like solute undergoing a monomer $\rightleftharpoons$ dimer association. The equilibrium constant (K_2) and the Huggins constant (k') were assigned values of 10 dl/g and 0.45, respectively.

the rotational frictional coefficient in terms of the axial ratio which is in excellent agreement with experiment

$$\text{torque}_{cyl} = \frac{8\,\pi\eta a^3\omega}{3\,[\ln(2a/b) - \gamma]} \tag{4}$$

where $\gamma = 1.57 - 7[(1/\sigma) - 0.28]^2$ for $\ln(2a/b) > 2$, $\sigma = \ln 2a/b$, a = half-length or semi-major axis, b = radius or semi-minor axis, η = viscosity of solvent, ω = angular velocity. The corresponding exact solution obtained by Perrin (1934) for a prolate ellipsoid is given by

$$\text{torque}_{ell} = \frac{8\,\pi\eta a^3\omega}{3\,[\ln(2a/b) - 0.5]} \tag{5}$$

To check the validity of the experimental approach employed in this investigation the rotational frictional coefficients of rods derived from torque measurements may be compared to those predicted by the Broersma equation. The results of this analysis are shown in Table I showing an excellent correlation between experiment and the Broersma equation over the range of axial ratios pertinent to the present study.

Rotational friction experiments on dimeric rod structures have been carried out for two systems with rods of different axial ratios corresponding to the monomeric LMM and rod particles. The results of these torque measurements are shown in Table II.

As there are no analytical solutions for the torque expected for rod dimer systems in terms of the particle geometry, we have proceeded as follows. Since the dimensions of the monomeric rod are known, it is possible to relate the volume of the dimer in terms of the half-length (a) and radius of the monomer (b).

$$\text{volume of dimer} = 4\pi ab^2 \tag{6}$$

Further, the length of the actual dimer is uniquely defined in terms of the half-length (a) of the monomer by the degree of overlap. Let us assume that we can replace the dimer by a cylinder having the same length and volume as the dimer

TABLE I: Comparison of the Reduced Rotational Coefficients (ζ/η) of Rods Obtained by Torque Measurements with Those Predicted by Broersma's Equation.

Axial Ratio	ζ/η (cm^3 rad^{-1}) Experimental	ζ/η (cm^3 rad^{-1}) Broersma	Ratio
43[a]	914	927	0.987
54[a]	1650	1690	0.974
75.9[a]	4170	4259	0.979
65[b]	1130	1142	0.990
87[b]	2500	2457	1.016
108[b]	4720	4519	1.044

[a] Diameter of stainless steel rod = 0.3174 cm. [b] Diameter of brass rod = 0.236 cm.

TABLE II: Reduced Rotational Frictional Coefficients (ζ/η) for Rod Dimer Structures.

Model	Fraction of Overlap	ζ/η Dimer (Experimental) (cm^3 rad^{-1})	$p_{eq\ cyl}$	$\zeta/\eta_{eq\ cyl}$ (Broersma) (cm^3 rad^{-1})	Ratio
LMM[a]	0.25	4200	71	4223	0.995
LMM[a]	0.50	2850	56	2856	0.998
LMM[a]	0.75	1790	43	1814	0.987
LMM[a]	1.0	1060	30.8	1051	1.011
ROD[b]	0.333	4690	99	4667	1.005
ROD[b]	0.666	2500	71	2624	0.953
ROD[b]	0.75	2100	64.5	2242	0.936
ROD[b]	1.0	1290	45.5	1281	1.005

[a] LMM monomer macromodel length 13.70 cm, diameter 0.3174 cm. [b] ROD monomer macromodel length 15.36 cm, diameter 0.236 cm.

under consideration. The axial ratio p_{cyl} of such a cylinder is readily deduced from the volume and length equality of cylinder to dimer. Thus, having obtained the axial ratio of this cylinder it is possible to calculate the rotational frictional coefficient expected for the effective cylinder by use of the Broersma formula (eq 4). This has been done for the cases corresponding to the dimer of LMM and rod and the results are shown in column 5 of Table II. It is immediately evident that this hydrodynamic substitution of the cylinder for the dimer, with the specific restrictions on volume and length, is an excellent one and appears to be valid for monomeric rods, at least for axial ratios (a/b) > 40, for all degrees of overlap.

We can now formulate, for rod-like particles undergoing dimerization, the relationship between dimer geometry and the intrinsic viscosity of the dimer. Consider a system comprised of homogeneous rods of length and diameter $2a$ and $2b$, respectively. Assume that these rods dimerize reversibly through side by side association and further, that only one specific dimer geometry is allowed.

The geometry of the dimer will be designated by a fraction of overlap, f, where the overlap distance, x (*i.e.*, the length of dimer congruent to both monomer units), is $2af$ and the extension, y, is, therefore, $2a - x = 2a(1 - f)$; the length of the dimer, $L = 2a(2 - f)$. Since it has been shown that the dimer is hydrodynamically equivalent to a cylinder of length and volume equal to that of the dimer, it is a simple matter to evaluate the axial ratio (p) for this cylinder in terms of the known parameters a, b, and f, as follows.

Let the radius of the cylinder be r. From the volume and length equality of cylinder to dimer it is easily shown that r is equal to $b[2/(2 - f)]^{1/2}$ and the axial ratio of the equivalent cylinder, $p_{eq\ cyl}$ is given by

$$p_{eq\ cyl} = \frac{2a(2 - f)}{2b[2/(2 - f)]^{1/2}} = [(2 - f)^3/2]^{1/2}(a/b) \qquad (7)$$

Thus, it is clear that the axial ratio of the equivalent cylinder and, therefore, that of the dimer of specific fraction of overlap, f, takes the form of a constant times the axial ratio of the monomer. The ratio of the axial ratio of the dimer to that of the monomer is given by

$$\frac{p_{eq\ cyl}}{p_{monomer}} = \left(\frac{(2 - f)^3}{2}\right)^{1/2} \qquad (8)$$

For the long prolate ellipsoids it can be shown that the viscosity increment, ν, is proportional to $p^{1.8}$ (Tanford, 1960) and assuming a similar relationship holds for ν of rods, the ratio of the dimer to monomer viscosity increment (ν_d/ν_m) is just $[(2 - f)^{3/2}/2^{1/2}]^{1.8}$. Assuming that the partial specific volume of the monomer and the dimer are the same

$$[\eta]_d = \frac{\nu_{eq\ cyl}}{\nu_{monomer}}[\eta]_m \qquad (9)$$

and

$$[\eta]_d = [(2 - f)^{3/2}/2^{1/2}]^{1.8}[\eta]_m \qquad (10)$$

Thus provided $[\eta]_m$ for a rod-like particle is known, the intrinsic viscosity of the dimer for any given degree of overlap is readily deduced or, *vice versa*, if both $[\eta]_m$ and $[\eta]_d$ are known the degree of overlap in the dimeric structure can be obtained with high precision independent of the absolute length of the monomer.

In the treatment above we have shown that dimeric structures of rods formed through side by side association can be hydrodynamically treated as equivalent cylinders of length and volume equal to that of the dimer. It is clear that a similar treatment where monomer and dimer are replaced by equivalent ellipsoids could also be carried out, but because of the difficulties involved in construction of ellipsoids of required geometry we have not verified this hydrodynamic substitution. We are reasonably certain that the same type of equivalence as found for the association of cylinders would prevail.

Determination of Dimer Geometry. In the preceding paper (Harrington and Burke, 1972) it was demonstrated that the reduced viscosity *vs.* concentration dependence of LMM and rod could be analyzed on the basis of a monomer $\rightleftharpoons$ dimer equilibrium to yield the intrinsic viscosity of the dimer. In order to determine the dimer geometries it was assumed that the dimers could be substituted hydrodynamically by equivalent prolate ellipsoids and the lengths (major axes) of these dimers (ellipsoids) were calculated on the basis of their intrinsic viscosities and molecular weights. These lengths for

TABLE III: The Relationship between Dimer Geometry and the Intrinsic Viscosity of the Dimer for Rod-Like Solutes.

Fraction of Overlap (f)	Equivalent Cylinder			$\frac{p_{eq\ cyl}}{p_{mon}}$	$\frac{\nu_{eq\ cyl}}{\nu_{mon}}$	$[\eta]_d$ (LMM)	$[\eta]_d$ (rod)	Length of Dimer (Å)	
	Length	Diameter	Axial Ratio					LMM[a]	Rod[a]
0 (monomer)	$2a$	$2b$	a/b			1.23	2.65	875	1380
1.0	$2a$	$2\sqrt{2}\,(b)$	$\frac{1}{\sqrt{2}}\,(a/b)$	0.709	0.538	0.66	1.43	893	1360
0.75	$5a/2$	$4\sqrt{\frac{2}{5}}\,(b)$	$\frac{5}{8}\sqrt{\frac{5}{2}}\,(a/b)$	0.989	0.980	1.22	2.60	1096	1720
0.666	$8a/3$	$2\sqrt{\frac{3}{2}}\,(b)$	$\frac{4}{3}\sqrt{\frac{2}{3}}\left(\frac{a}{b}\right)$	1.09	1.168	1.44	3.10	1169	1840
0.5	$3a$	$\frac{4}{\sqrt{3}}\,(b)$	$\frac{3\sqrt{3}}{4}\,(a/b)$	1.296	1.596	1.96	4.23	1320	2075
0.333	$10a/3$	$2\sqrt{\frac{6}{5}}\,(b)$	$\frac{5}{3}\sqrt{\frac{5}{6}}\,(a/b)$	1.525	2.138	2.63	5.66	1477	2310
0.25	$7a/2$	$2\sqrt{\frac{8}{7}}\,(b)$	$\frac{7}{4}\sqrt{\frac{7}{8}}\left(\frac{a}{b}\right)$	1.625	2.399	2.95	6.35	1547	2410
0 (dimer)	$4a$	$2b$	$2(a/b)$	2.00	3.475	4.27	9.20	1750	2760

[a] Values for the molecular weights were 122,000 (LMM) and 198,000 (rod) (Harrington and Burke, 1972). Length is calculated from the equation $L = 6.82 \times 10^{-8}([\eta]M)^{1/3}(p_e^2/\nu_e)^{1/3}$ (Yang, 1961).

the dimers of LMM and rod taken together were found to be consistent with a parallel geometry for the parent myosin dimer.

The present investigation has demonstrated that the hydrodynamic substitution of an equivalent cylinder for the dimer, with length and volume equal to the dimer, is an excellent one for all degrees of overlap and, therefore, the assumption that $\text{length}_{\text{cylinder}} \simeq \text{length}_{\text{ellipsoid}}$ for large axial ratios employed in the previous paper is reasonable. It can be seen that eq 10 may be used to determine the fraction of overlap for dimers of rod-like particles provided both $[\eta]_d$ and $[\eta]_m$ are known. Applying this analysis to the viscosity data summarized in Table II of the previous paper we find that the fractions of overlap for LMM and rod dimers are 0.50 and 0.60, respectively, in agreement with estimates from monomer and dimer lengths evaluated in the preceding paper (Table III, Harrington and Burke, 1972). These findings are consistent, therefore, in assigning a parallel geometry to the myosin dimer in which one unit is displaced between 430 and 530 Å with respect to the other.

It is of interest to note that if the geometries of the dimers of LMM and rod were fully overlapped the expected intrinsic viscosities would be 0.66 and 1.43 dl per g, respectively (Table III), values approximately one-half those of their corresponding monomers. The reduced viscosity *vs.* concentration profile of a monomer reversibly associating to a fully overlapped dimer would, therefore, take the form of the plot shown in Figure 2b. This behavior is at variance with the experimental findings for these particles (Harrington and Burke, 1972).

Although the above study provides evidence that the myosin dimer existing at high ionic strength is a parallel structure, it was of interest to examine whether this conclusion could be supported by an investigation of the hydrodynamic properties of macromodels corresponding to the monomer and dimer species of myosin. The nonsymmetrical mass distribution in the myosin molecule places restrictions on models which may be used and also precludes employment of standard hydrodynamic methods for analysis of the data. In the following section we describe rotary frictional experiments on macromodels corresponding to myosin and the procedures we have employed for analysis of the hydrodynamic data.

Macromodels Corresponding to Myosin. The most generally accepted structure for myosin is a uniform, rigid rod terminating in two globular regions at a common extremity with the mass of the molecule divided approximately equally between the rod section, on the one hand, and the two globular regions on the other (Slayter and Lowey, 1967; Lowey *et al.*, 1969). To account for the uneven mass distribution in myosin, we have chosen a simplified model for this molecule comprising a rod attached at one end to a sphere with the same volume as the rod. Although this model is a rather crude approximation of the actual molecule, its hydrodynamic properties are not expected to be grossly dissimilar since the flow properties reflect a geometric envelope (Broersma, 1960) and should be rather insensitive to the fine detail of the head structure.

In a viscous medium a particle will rotate about an axis perpendicular to the long axis of the model, where the torque required to rotate the particle with unit angular velocity is a minimum and this torque is the rotational frictional coefficient. The point of rotation for minimum torque is not in general the center of gravity for a model with nonuniform mass distribution, since the frictional resistance will not be symmetrical about the center of gravity of the particle (we thank Dr. B. H. Zimm for pointing this out to us). The axis of minimum torque of the myosin model was determined from a series of torque measurements about different rotational axes along the length of the model. These experiments indicate that the minimum torque (1570 $cm^3\ rad^{-1}$) is located at a position $0.595L$ from the free rod extremity, where L is the length of the rod. The problem remaining is to relate this minimum torque to an intrinsic viscosity.

The first procedure adopted was to relate the experimentally determined minimum torque to an equivalent prolate ellipsoid. Using this information and the volume equality of

TABLE IV: Hydrodynamic Parameters Evaluated for Monomeric and Dimeric Myosin from Rotary Frictional Experiments on Macromodels.

Structure	$[\eta]^a$ (dl/g)	$[\eta]^b$ (dl/g)	ζ^d (dyne cm sec)	θ^d (sec^{-1})
Myosin (monomer)	1.57	2.29 (2.45)[c]	1.41×10^{-17}	2720
Myosin (parallel dimer)	1.74	2.57 (3.11)[c]	3.04×10^{-17}	1260
Myosin (antiparallel dimer)	3.94	6.01	6.82×10^{-17}	563

[a] For rod length 1290 Å. [b] For rod length 1440 Å. [c] Values in parentheses are those evaluated from viscosity measurements on solutions of these proteins. [d] Expected value for the rotational diffusion coefficient (θ) based on rotary frictional coefficients on macromodels and employing a linear magnification factor of 1.91×10^6, evaluated for system in water at 5°.

ellipsoid to macromodel the axial ratio was calculated from eq 4. This analysis yields an axial ratio of approximately 47.5 corresponding to a viscosity for the myosin monomer of about 1.2 dl/g, a value much lower than that observed experimentally ($[\eta]_m$ = 2.45 dl/g). Two factors may be contributing to this discrepancy. First, an incorrect geometry (*e.g.*, the length and diameter of the rod) of the model may have been assumed and second, the inadequacy of the substitution of a symmetrical ellipsoid for a nonsymmetrical particle. In view of the large divergence between the predicted and observed viscosity an alternative approach based on a modification of the string of beads procedure (see, for example, Mark and Tobolsky, 1950; Riseman and Kirkwood, 1950) was chosen. This analysis is more readily adapted to the model under consideration since the frictional asymmetry can be weighted appropriately from the assumed three-dimensional geometry.

In this treatment the total torque on the model is considered to arise from two separate contributions stemming (1) from the frictional resistance experienced by the rod segment of the model rotated about the axis of minimum torque of the *myosin model* and (2) from the globular head of the model rotated about this same axis. Experiments carried out by rotation of the model about its *center of gravity* indicate that approximately 90% of the torque is contributed by the rod segment of the model under this condition. The contribution of the rod segment to the total torque is, however, more properly evaluated, as we have noted above, from torque measurements on this segment *alone* rotated about the axis of minimum torque of the myosin macromodel. This torque may then be related to a virtual equivalent cylinder or equivalent prolate ellipsoid with volume equal to the rod according to eq 4 and 5. The volume equality is a necessary requirement from the definition of intrinsic viscosity. Since there is an exact relationship between the viscosity increment (ν) and axial ratio (p_x) of an equivalent prolate ellipsoid (Simha, 1945) we have related this torque to a virtual prolate ellipsoid.

The viscosity contribution of the sphere spun about the axis of minimum torque of the myosin model is readily evaluated from the string of beads method and is given by eq 11

$$\eta_{sp}/c = \frac{\pi(a)(r + a)^2 N}{100M} \qquad (11)$$

where a = Stokes radius of the sphere, r = distance from center of rotation to surface of sphere, N = Avogadro's number, M = molecular weight of sphere. We assume the intrinsic viscosity of the model is given by the sum of the products of the viscosity contribution of each segment times the volume fraction occupied by that segment.

The analysis has been carried out for particles corresponding to rod lengths of 1290 and 1440 Å with constant diameter of 20 Å, attached to spheres of radii 45.9 and 47.6 Å, respectively. The contributions to the intrinsic viscosity of the rod section and the sphere were calculated to be 1.92 dl/g and 1.22 dl/g, respectively, for the particle with the 1290-Å rod section and 3.0 dl/g and 1.57 dl/g for the particle with the 1440-Å rod. The results are shown in Table IV from which it can be seen that the analysis based on the model with the 1440-Å rod section is in reasonable agreement with the experimental findings for myosin.

For dimeric myosin the two general types of structures, parallel and antiparallel, must be considered. In the case of the antiparallel dimer the mass and the frictional resistance are both distributed symmetrically about the center of gravity. This property allows us to calculate immediately the contributions of the rod segment and the spheres. The rod contribution for any degree of overlap may be calculated from eq 10 and eq 11 is used to calculate the contribution of each sphere. For the parallel-type dimers the center of gravity is not the center of frictional resistance and, therefore, this system is subject to the same considerations described for the monomeric particle with respect to the location of the rotation axis. Since we have demonstrated the hydrodynamic equivalence of the rod dimer and a cylinder of the same length and volume, the contribution to the total torque will be given by rotation of this equivalent cylinder about the point of minimum torque of the dimer myosin model. The viscosity increment and intrinsic viscosity contributed by the rod section of the dimer is evaluated as in the case of the myosin monomer. The viscosity contribution of each sphere is obtained from eq 11 since its distance from the point of rotation is also known.

We have evaluated the intrinsic viscosity expected for parallel and antiparallel myosin dimers corresponding to a 430-Å displacement and a 430-Å overlap, respectively. These models were chosen because of the well-defined geometry established for the LMM dimer. Rotary frictional experiments on macromodels corresponding to the parallel dimer of myosin have indicated that the rotation axis of minimum torque (3380 cm^3 rad^{-1}) occurs at 0.575L from the rod extremity, where L in this case is the total length of the rod segment of the dimer. The results of this analysis are presented in Table IV for the two different assumed monomeric rod lengths, 1290 and 1440 Å. The intrinsic viscosity evaluated from the macromodel of the parallel dimer is in reasonable agreement with the computed value from the myosin data, whereas that for the antiparallel structure is clearly much too high. Although other geometries of the myosin dimer may be consistent with the experimentally observed value of $[\eta]_d$ (for example, an antiparallel structure associating by overlap

of the subfragment II sections) they can be eliminated on the basis of our findings on the geometry of the LMM and rod dimers.

Acknowledgments

We would like to thank Mr. Z. H. Schroeder of the Instrument Workshop, for the skillful construction of the apparatus and models used in the hydrodynamic experiments.

References

Broersma, S. (1960), *J. Chem. Phys. 32*, 1626.
Burgers, J. M. (1938), *Verhandel. Koninkl. Ned. Akad. Wetenschap. 16*, 113.
Haltner, A. J., and Zimm, B. H. (1959), *Nature (London) 184*, 265.
Harrington, W. F. and Burke, M. (1972), *Biochemistry 11*, 1448.
Kuhn, H., and Kuhn, W. (1952), *J. Polym. Sci. 9*, 1.
Lowey, S., Slayter, H. S., Weeds, A. G., and Baker, H. (1969), *J. Mol. Biol. 42*, 1.
Mark, H., and Tobolsky, A. V. (1950), Physical Chemistry of High Polymeric Systems, New York, N. Y., Interscience, p 291.
Perrin, F. (1934), *J. Phys. Rad. 5*, 497.
Reisler, E., and Eisenberg, H. (1970), *Biopolymers 9*, 877.
Riseman, J., and Kirkwood, J. G. (1950), *J. Chem. Phys. 18*, 512.
Simha, R. (1945), *J. Chem. Phys. 13*, 188.
Slayter, H. S., and Lowey, S. (1967), *Proc. Nat. Acad. Sci. U. S. 58*, 1611.
Tanford, C. (1960), Physical Chemistry of Macromolecules, New York, N. Y., Wiley, p 335.
Yang, J. T. (1961), *Advan. Protein Chem. 16*, 323.

Evidence for Cis Peptide Bonds in Copolypeptides of Glycine and Proline†

D. A. Torchia

ABSTRACT: Poly(Pro-Gly) and poly(Gly-Gly-Pro-Gly) have been examined using 220-MHz nuclear magnetic resonance (nmr) spectroscopy. The data indicate that the two polypeptides have unordered structures in trifluoroethanol, dimethyl sulfoxide, and aqueous solution. However, the spectra of both sequential copolypeptides show two resonances, having unequal areas, for individual Gly NH protons and Pro α protons. Evidence is presented which shows that these resonances result from the presence of both cis and trans Gly–Pro peptide bonds "randomly" distributed in a given polypeptide chain. The observed temperature dependence of the relative population of the two isomers in water yields approximate values of the enthalpy and entropy difference between the cis and trans isomers. Solvent also influences the relative population of the isomers, with the fraction of cis bonds in poly(Pro-Gly) decreasing from 0.4 to 0.2 (at 22°) on going from dimethyl sulfoxide to aqueous solution. Solvent effects on line widths and NH chemical shifts suggest that the flexibility of the polypeptide backbone and the solvent accessibility of Gly NH protons are solvent dependent. In the light of these results, the conformational characteristics of naturally occurring polypeptides containing proline are discussed.

Recent nuclear magnetic resonance (nmr) studies (Madison and Schellman, 1970; Deber *et al.*, 1970; Torchia *et al.*, 1972a,b) have shown that linear and cyclic oligopeptides containing Pro[1] residues maintain multiple conformations in solution distinguished by different isomers (cis and trans) of X-Pro peptide bonds. Except for poly(Pro) itself, cis peptide bonds have not been reported in solution for polypeptides containing Pro residues. In addition to having possible biological applications, the observation of cis X-Pro peptide bonds in polypeptides and measurement of effects of solvent and temperature on the population of cis isomers would be useful in aiding interpretation of optical and hydrodynamic data. Also, such results can be used to check calculated polypeptide conformational energies. High-frequency nmr is ideally suited to detect the presence of cis and trans peptide isomers. The barrier to cis $\rightleftarrows$ trans interconversion is sufficiently high so that rotation about the peptide bond is slow and separate resonances, corresponding to the two isomers, can be detected directly (Torchia and Bovey, 1971).

For these reasons we have chosen to study poly(Pro-Gly) and poly(Gly-Gly-Pro-Gly) using 220-MHz nmr. A previous study (Mattice and Mandelkern, 1970, 1971a,b) of these polymers, using optical and hydrodynamic techniques, has shown that they are unordered in trifluoroethanol and aqueous solution. In the unordered state, rapid rotation about the single bonds in the polypeptide backbone occurs which results in averaging out of direct dipolar interactions. Thus, high-resolution spectra, which greatly simplify analysis, are

† From the Bell Laboratories, Murray Hill, New Jersey. Current address: Polymers Division, National Bureau of Standards, Washington, D. C. 20234. *Received September 13, 1971.*

[1] The following abbreviations will be used in this paper: Gly for glycyl; Pro for L-prolyl; Ser for L-seryl; Sar for sarcosyl; X for any amino acid residue except prolyl; *t* for temperature; DP for degree of polymerization; Me_4Si for tetramethylsilane; Me_2SO-d_6 for hexadeuteriodimethyl sulfoxide.